ELSEVIER

Palaeogeography, Palaeoclimatology, Palaeoecology 170 (2001) 219–236

PALAEO

www.elsevier.nl/locate/palaeo

CO_2 levels in the Late Palaeozoic and Mesozoic atmosphere from soil carbonate and organic matter, Satpura basin, Central India

Prosenjit Ghosh[a,*], P. Ghosh[b], S.K. Bhattacharya[a]

[a]*Earth Science Division, Physical Research Laboratory, Navrangpura, Ahmedabad 380 009, India*
[b]*Geological Studies Unit, Indian Statistical Institute, 203, B.T. Road, Calcutta 700 035, India*

Received 12 October 1999; accepted for publication 13 February 2001

Abstract

A number of calcic palaeosols have been identified within the fluvial deposits of the Motur (Permian), the Denwa (Triassic), the Bagra (Jurassic) and the Lameta (Cretaceous) Formations of the Satpura sedimentary succession, Central India. These palaeosols show accumulation of pedogenic carbonates in rhizocretions and glaebules. The carbon isotopic compositions of these carbonates and the coexisting soil organic matters are used to determine the isotopic composition and the partial pressure of atmospheric CO_2 using the CO_2 palaeobarometer developed by Cerling [Am. J. Sci., 291 (1991) 377]. It is seen that the atmospheric CO_2 level increased by a factor of 8 from the Permian to the Jurassic and declined again during the Cretaceous. The nature of the changes agrees with the result of the CO_2 evolution model of Berner (GEOCARB II) but the magnitude of the CO_2 increase in the Middle Jurassic and the Late Cretaceous was higher than the predicted value. Degassing of Earth's interior due to rapid break-up of the Gondwana landmass during the Triassic and Jurassic period could have caused the rapid CO_2 increase.

Keywords: Gondwana; Palaeosol; Carbon dioxide evolution

1. Introduction

Carbon dioxide (CO_2) is one of the major greenhouse gases in the Earth's atmosphere and changes in the atmospheric concentration of CO_2 (pCO_2) can significantly influence the Earth's surface temperature (Houghton and Wood, 1989) leading to major changes in climate, surface processes and biota. Over the last two centuries combustion of fossil fuels have raised the atmospheric CO_2 level from about 275 ppmV (Barnola et al., 1987) to the current level of 365 ppmV (Keeling et al., 1989; Keeling and Worf, 1998; Keeling, 1994). From the analysis of trapped gases in the polar ice-cores Barnola et al. (1987) showed that during the past 150,000 years CO_2 level had oscillated between ~200 and 300 ppmV. Similarly, $\delta^{13}C$ analysis of pedogenic carbonates and stomatal index count of fossil leaves provide evidence for large variations in pCO_2 in geologic past (Cerling, 1991; Ghosh et al., 1995; Mora et al., 1996; McElwain and Chaloner, 1996; Ekart et al., 1999). Theoretical models of the carbon cycle based on mantle evolution (Tajika and Matsui, 1992) and biological and tectonic changes in the past (Berner, 1991, 1993, 1994 and 1997) also predict large changes in the atmospheric pCO_2 during the Phanerozoic. For example, the GEOCARB II model of Berner (1994) predicts that in the Early Phanerozoic (550 Ma) the pCO_2 was 20 times the present atmospheric level

* Corresponding author. Fax: +91-79-6301502.
E-mail address: pghosh@prl.ernet.in (P. Ghosh).

0031-0182/01/$ - see front matter
PII: S0031-0182(01)00237-1

(PAL). Subsequently, the pCO_2 declined in the Middle and Late Palaeozoic (450–280 Ma) to reach a minima (approximately similar to the PAL) at about 300 Ma. The period 300–200 Ma was again characterised by a rapid rise when the pCO_2 increased to 5 times the PAL. It was followed by a gradual decline to the PAL with a small peak in the Early Tertiary. Such large changes in pCO_2 in the geologic past must have had significant influences on the climate, biota and surface processes of the Earth (Berner, 1991, 1997; Mora et al., 1996). Therefore, understanding the nature of variation in atmospheric pCO_2 is important for a better reconstruction of the Earth's physical and biotic history.

The purpose of this study is to supplement the global database of palaeo-pCO_2 levels for parts of Late Palaeozoic and Mesozoic using a palaeosol CO_2 palaeobarometer (Cerling, 1991). The stable isotopic composition of pedogenic carbonates of the calcic palaeosols developed in the Gondwana succession and associated sediments of Central India has been investigated in this study. The carbon isotopic composition of the organic matter associated with these carbonates has been used to estimate the isotopic composition of the atmospheric CO_2 and the plant-respired CO_2 during periods of soil formation. These estimates may be used to constrain a part of the Phanerozoic pCO_2 history.

2. Study area and samples

The Gondwana sediments and the overlying Deccan trap of the Satpura basin of Central India range in age from the Permo-Carboniferous to the Late Cretaceous. The thickness of the whole sedimentary succession is about 5 km (Fig. 1). The sediments comprise alternate layers of coarse clastics (sandstones along with extrabasinal conglomerates) and fine clastics (red mudstone/carbonaceous shale/ white mudstone). The basal unit of this succession is a Permo-Carboniferous glacio-lacustrine deposit, the Talchir Formation. The formations overlying the Talchir represent several episodes of fluvial, lacustrine and alluvial deposition (Robinson, 1967; Casshyap and Qidwai, 1971; Casshyap and Tewari, 1988; Casshyap et al., 1993; Veevers and Tewari, 1995; Ghosh, 1997). Occurrences of fossil vertebrates (Chatterjee and Roychowdhury, 1974; Mukherjee and Sengupta, 1998; Bandyopadhyay and Sengupta, 1998) and fresh-water bivalves, coupled with evidences of pedogenesis, like the presence of rootlet horizons, palaeosol profiles etc. (Ghosh et al., 1995, 1998; Ghosh, 1997; Tandon et al., 1995, 1998) support the alluvial origin of these sediments.

In four litho-formations (Motur, Denwa, Bagra and Lameta Formations) of the Satpura sedimentary succession preserved calcic palaeosols have been identified (Ghosh et al., 1995, 1998, Ghosh, 1997; Tandon et al., 1995, 1998; Andrews et al., 1995). The respective ages of these Formations are Early Middle Permian (260 Ma), Middle Triassic (240 Ma), Jurassic (200 Ma) and Late Cretaceous (65 Ma) (Chatterjee and Roychowdhury, 1974; Raja Rao, 1983; Satsangi, 1988; Casshyap et al., 1993; Bandopadhyay and Sengupta, 1998). The pedogenic carbonates and associated organic matters from these Formations were analysed for stable isotopes. We also analysed the carbon isotopic composition of the organic matter associated with the palaeosol samples of the Lameta Formation collected earlier (see Ghosh et al., 1995 for details of the Lameta samples).

2.1. Motur Formation

The Motur Formation is a 400–700 m thick succession of fluvial channel sandstone bodies alternating with floodplain complexes made up of red claystone and thin sandy splay deposits. In the middle part of the Motur succession a few calcic palaeosols occur within the floodplain deposits. These palaeosols are characterised by three to four vertically superposed distinct pedo-horizons forming palaeosol profiles (Fig. 2(a)). Two types of profiles can be recognised. One type is around 50 cm thick, whereas the other is thicker (3–4 m). The thinner variety comprises an uppermost horizon (3–5 cm thick) of coalesced platy glaebules (Fig. 2(b)) overlying a 10–30 cm thick horizon of closely spaced vertically oriented rhizocretions. The rhizocretion horizon grades downward to a horizon with profuse sub-spherical glaebules that overlies a gleyed horizon. The uppermost horizon of fused platy glaebules is similar to the K horizon of modern aridisols whereas the zones of rhizocretions and glaebules can be compared with the Bk soil horizons (Soil Survey Staff, 1975).

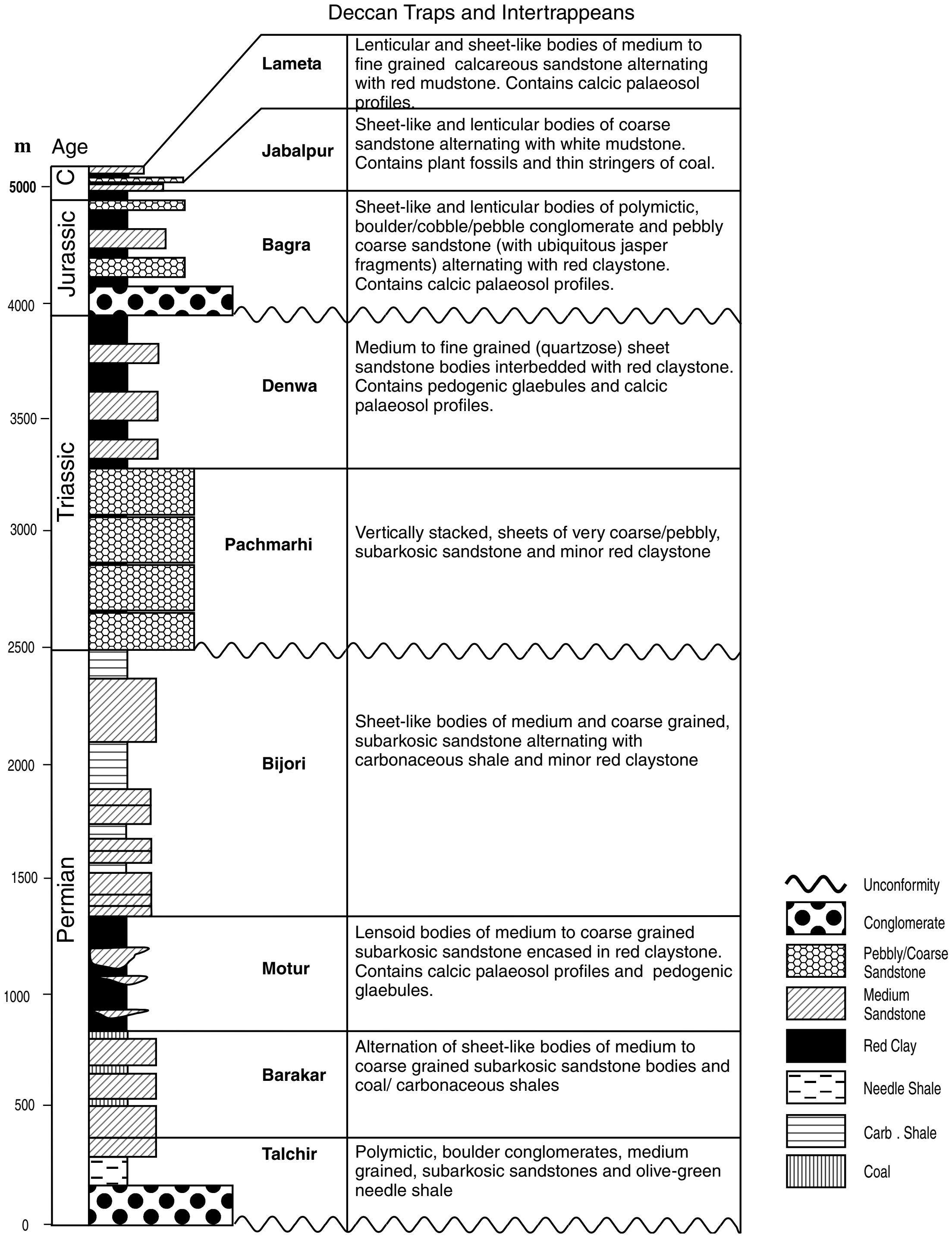

Fig. 1. Generalised lithostratigraphy of the Gondwana succession of the Satpura Basin.

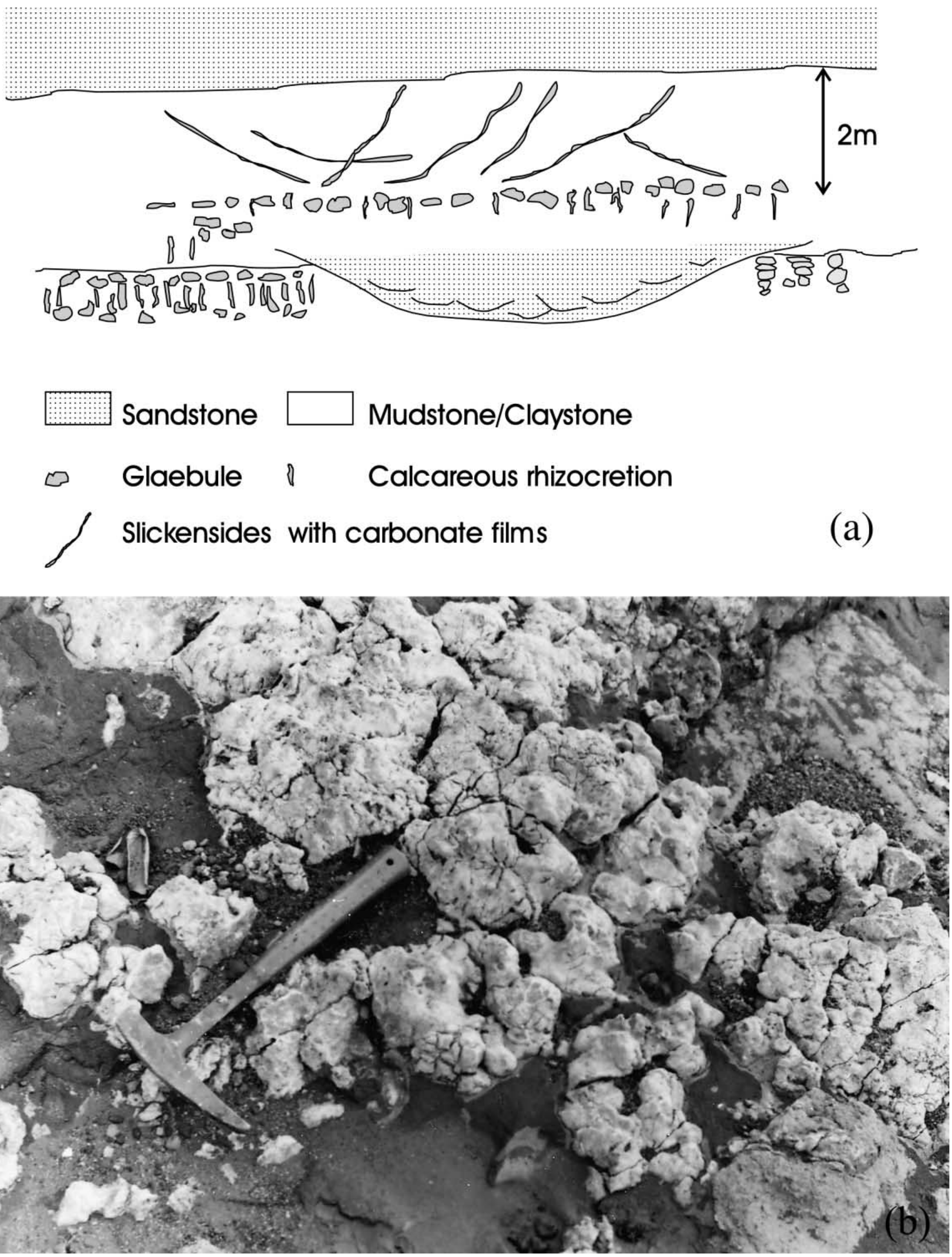

Fig. 2. (a) Field sketch of two vertically superposed calcic palaeosol profiles of the Motur Formation, exposed near Eklahara colliery; (b) Close up view of glaebular horizon (top surface view).

The thicker palaeosol profiles show a metre thick upper zone with a number of curved, mutually intersecting inclined zones (Fig. 2(a)), filled with centimetre thick carbonate precipitates, within a red claystone host. These zones resemble pedogenic slickensides (ss horizon) that develop in modern vertisols in response to shrinking and swelling of the soil clay matrix (Soil Survey Staff, 1975; Tandon et al., 1998). The underlying horizon is characterised by small, sub-vertical, dispersed, calcareous rhizocretions within a claystone host. This horizon is underlain by a thin (3–5 cm thick) layer of sub-spherical glaebules overlying a gleyed horizon (~20 cm thick). These features can be compared with modern Bk horizons. The field features of these palaeosols are similar to the Appalachian Palaeozoic vertic palaeosol profiles described by Driese and Mora (1993) and Mora et al. (1998).

A total of 21 samples were collected from the palaeosol profiles of the Motur Formation near Eklahara colliery (Lat. 22°12′N and Long. 78°41′E). For the thinner palaeosols samples of rhizocretions and glaebules were collected from the basal part of the horizon. The upper horizons of platy glaebules were not sampled to avoid anomalous contribution of atmospheric CO_2 near the soil–atmosphere contact as explained below.

Studies on vertic palaeosols have demonstrated that the glaebules occurring within the vertic horizons are enriched in ^{13}C compared to those occurring below the vertic horizons and from the rhizocretions in general (Driese and Mora, 1993; Mora et al., 1993). Vertisols have both pedogenic slickensides (formed by shrinking and swelling of soil clay matrix) and wedge-shaped vertical cracks formed by dessication. These latter cracks often intersect the soil surface and may allow direct and non-diffusive penetration of heavier atmospheric CO_2 deeper down the soil; hence samples from this horizon may produce anomalously high concentration of atmospheric CO_2.

2.2. Denwa Formation

The Denwa Formation is 300–600 m thick. The lower half of the Formation is characterised by a regular alternation of medium to fine-grained, thick (3–15 m) fluvial channel sandstone bodies and floodplain deposits. The floodplain deposits comprise red mudstones intercalated with centimetre to decimetre thick, fine-grained sandstone layers. In contrast to the lower part of the Formation, its upper-half is fines-dominated. The red mudstones encase 2–4 m thick, fine-grained (fine sandstones and siltstones) point bar deposits and about a metre thick lenticular channel-fill bodies. Pebble to coarse-sand sized detrital sub-spherical glaebules constitute the bulk of these channel-fill bodies. These bodies are internally trough cross-stratified (Fig. 3(a)).

The field occurrence of palaeosols in the Denwa Formation is limited and only wide spread occurrence of detrital glaebules with pedogenic micro-fabrics provides indirect evidence of pedogenesis during the later part of the Denwa sedimentation (Maulik et al., 2000). However, exposed palaeosol with two distinct pedo-horizons can be studied in a single exposure (Fig. 3a). This profile is more than 4 m thick. Its upper 2–3 m is characterised by a number of inclined and mutually intersecting planer features and dispersed small pebble to coarse sand sized glaebules and pale yellow blotches. Larger inclined features are about 5 m long and 5–7 cm thick whereas the length of the smaller ones is 1–2 m and these are less than a centimetre thick. Large inclined features are filled with calcareous silt. The surfaces of the smaller inclined features have a polished appearance and are, at places, coated by 1–5 mm thick carbonate layers. This horizon passes gradually to an underlying horizon of isolated pebble size glaebules, small (2–7 cm long) calcareous rhizocretions and pale yellow grey mottles. The larger inclined features of the overlying horizon, however, cut across the lower horizon. The smaller inclined features may possibly be equated with the pedogenic slickensides noted in the upper part of the modern day vertisols (Soil Survey Staff, 1975). The lower horizon represents the zone of carbonate accumulation at a deeper part of the soil. The discordant relationship between the pedo-horizons and the large inclined features along with their silty fills suggest that these are possibly desiccation cracks. The desiccation cracks, in vertisols is expected to be sub-vertical rather than inclined. However, in the present situation compaction of the Denwa sediments might have reduced the inclination of the steeply inclined desiccation cracks. The micro-fabric of both the detrital and the insitu glaebules are similar but the outlines of the detrital glaebules are

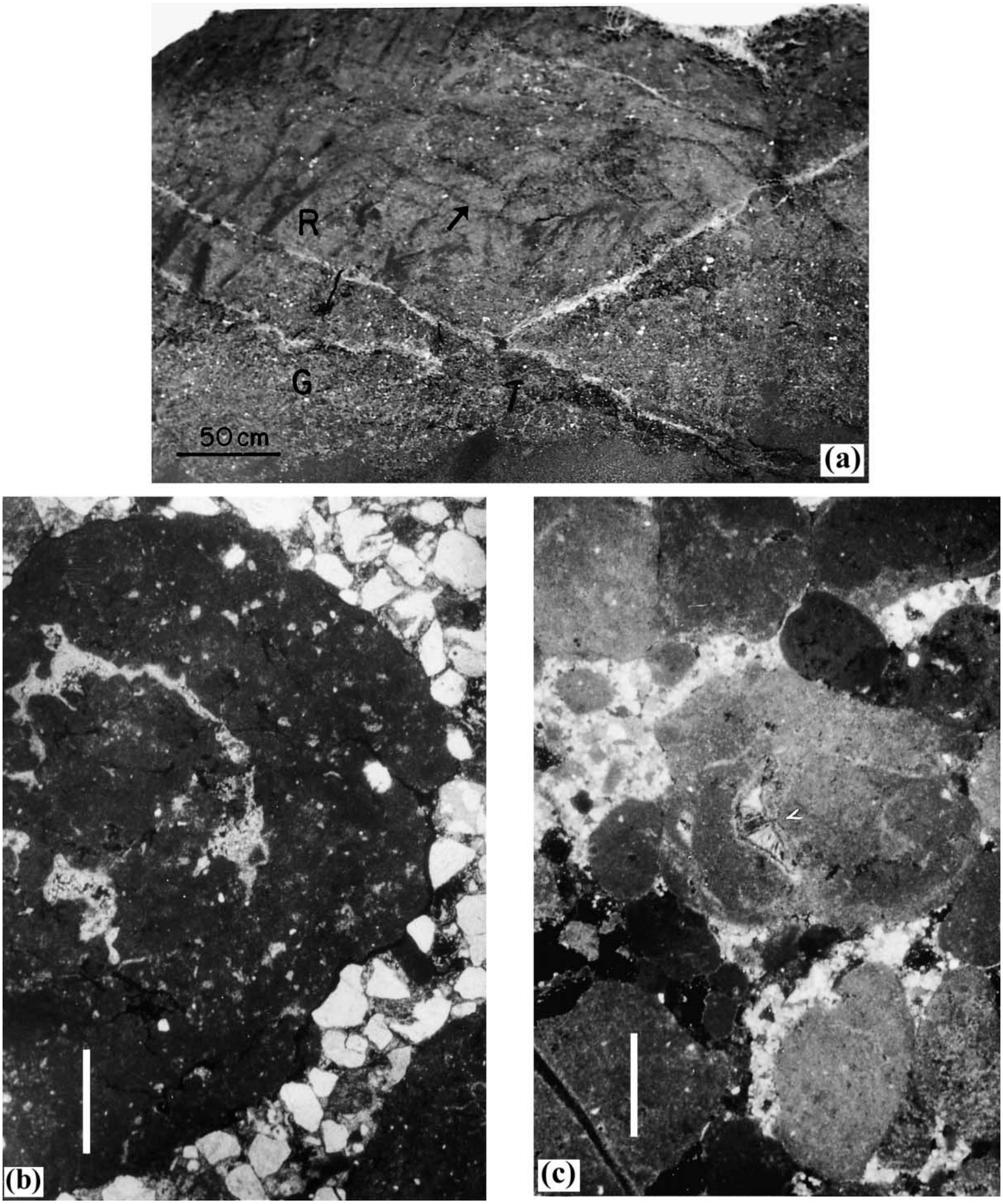

Fig. 3. (a) A vertic palaeosol profile of the Denwa Formation, exposed near Taldhana village. Note the presence of large, inclined dessication cracks (with a light coloured fill) along with darker and thinner inclined pedogenic slickensides (arrow) in the upper part. Some of the white dots are mottles. Hammer for scale. (b) Photo-micrograph showing part of a detrital glaebule. Note the sharp and rounded outline of the glaebule and the spar-filled (lighter) circum-granular crack (Scale bar is 1 mm); (c) Photo-micrograph of pedogenic glaebule. Note barite filled arcuate fracture in one of the glaebule (near the centre of the photograph). Oblique polars view. (Scale bar 0.8 mm).

sharp and rounded (Fig. 3b) whereas those of the insitu glaebules are diffused. Both the types of gleabules are mostly composed of micrite and minor microspar with one or two sand sized detrital quartz grains floating in the carbonate groundmass (Fig. 3b). A number of glaebules show radial fractures filled with either blocky spars or barite. Spar-filled, circum-granular cracks have also been noted in some of the glaebules along with pedogenic features like clotted micrite and corroded detrital quartz grains (Fig. 3b and c).

19 samples of soil carbonates were collected from the Formation. The bulk of the samples comprise detrital pedogenic glaebules of the channel-fill bodies (between Lat. 22°38′N and 22°35′N and Long. 78°20′E and 78°38′E). The rhizocretions and glaebules from the basal horizon of the palaeosol near Taldhana village (Lat. 22°37′N, Long. 78°32′30″E) were also sampled.

2.3. Bagra Formation

The Bagra Formation is 250–500 m thick. Thick units of polymictic conglomerates and pebbly sandstones, interbedded with red claystone units characterise this Formation. The internal architecture of the clastic bodies indicates that most of them were deposited within the channels of braided streams whereas the claystones were formed in the associated floodplains. The palaeosol profiles are mostly associated with these floodplain deposits and are found in the lower half of the Formation. At places, pedogenic modification extended up to the coarse grained abandoned channels and the wings of the main channel bodies. The palaeosol profiles are 70 cm–2 m thick. They are characterised by 10–50 cm thick well-developed horizon of fused calcareous glaebules at the top (Fig. 4(a)). A thick to very thick (50 cm–1.5 m) horizon of closely spaced, vertically oriented, large cylindrical rhizocretions occurs below the top glaebule horizon. The cross-sectional diameter of the rhizocretions ranges from 3 to 5 cm and the length ranges from 30 to 100 cm. The rhizocretions internally show two distinct co-axial cylindrical regions with a sharp contact in between (Fig. 4(b) and (c)). The inner region (1–2.5 cm in cross-sectional diameter) comprises large spars and minor carbonaceous clays (Fig. 4(c)). The outer region is made up of reddish grey micritic limestone. The field features of the palaeosol profiles of the Bagra Formation are comparable to the present day aridisols with a well-developed K-horizon at the top and a thick Bk horizon below it (Soil Survey Staff, 1975).

A total of 29 samples from the rhizocretions and pedogenic glaebules were collected from different palaeosol profiles of the Bagra Formation between Lat. 22°35′N and 22°40′N and Long.78°18′E and 78°37′30″E.

3. Experimental procedure

The application of Cerling's CO_2 paleobarometer requires analysis of carbonates formed during pedogenesis at a depth greater than 20 cm in the soil profile such that CO_2 transport is governed by diffusion. In this context, the thin sections of the samples were observed under petrographic mircoscope to identify portions rich in micrites which are most likely pedogenic in origin. In contrast, spar filled portions represent groundwater or diagenetic cements and were carefully avoided. Micritic portions of a section were sampled using a dental drill. XRD analysis of sample powders shows dominance of calcite with subordinate clays and minor quartz. Few milligrams of powder were reacted with 100% orthophosphoric acid at 50°C in vacuum using an online extraction system (Sarkar et al., 1990). The evolved CO_2 was thoroughly purified before analysing it in a VG 903 mass spectrometer. Some of the samples were analysed in a GEO 20-20 dual inlet mass spectrometer using an online CAPS (Carbonate Preparation System) system at 80°C. Samples were analysed along with NBS-19 and Z-Carrara (Internal Laboratory standard) for calibration and check-up of the system.

In order to determine the $\delta^{13}C$ value of organic matter associated with the soil carbonates, powdered samples were treated with 20% HCl for 24 h to remove the carbonates. Dried residue was loaded in a 10-cm long quartz break seal tube along with CuO (wire form) and silver strip. Quartz tube was evacuated, sealed and combusted at 700°C for 6 h. Evolved CO_2 was purified and analysed using GEO 20-20 IRMS. To check the reproducibility of measurements, UCLA glucose standard was analysed along with each

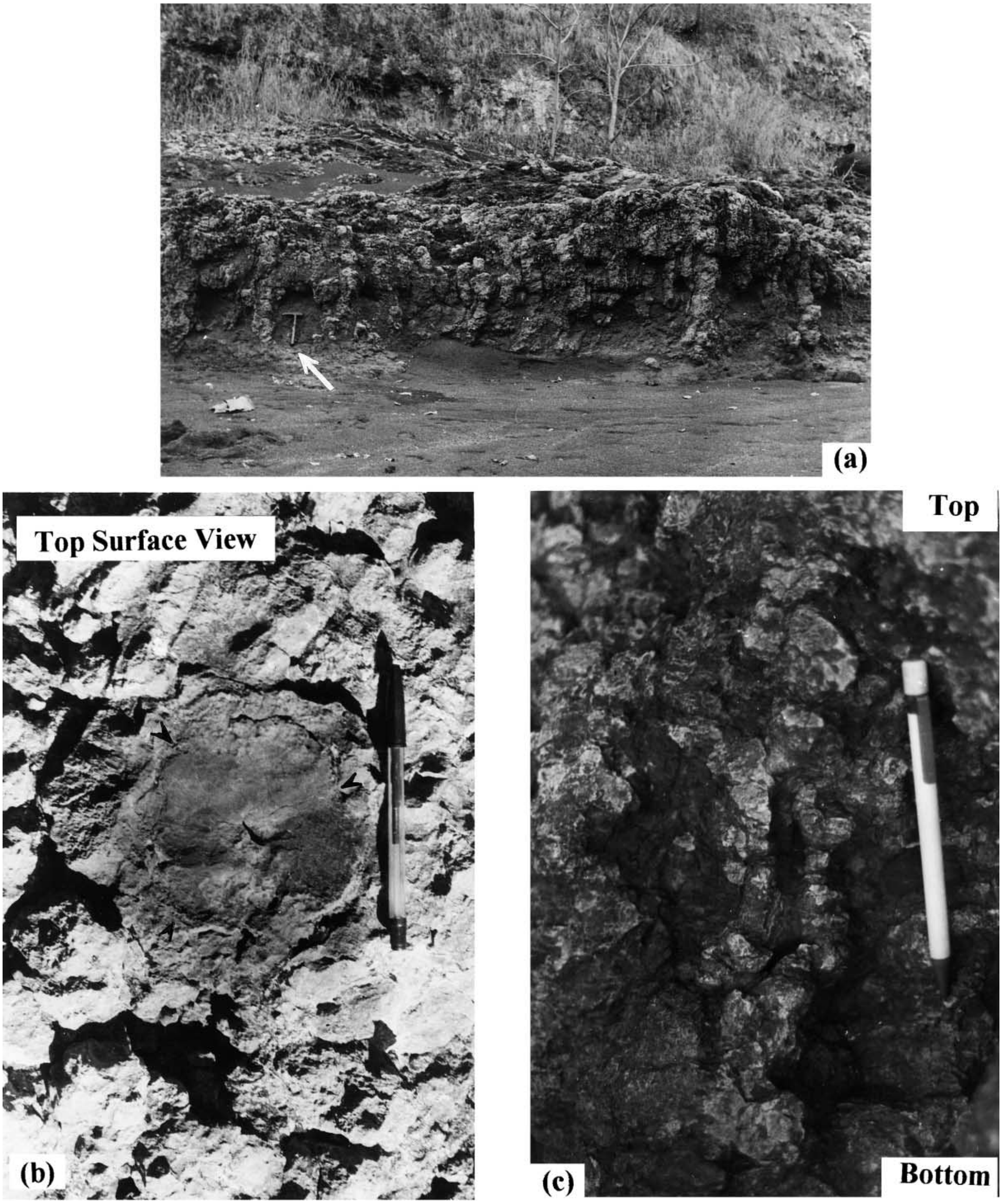

Fig. 4. (a) A calcic palaeosol profile of the Bagra Formation. Note a horizon of coalesced glaebules in the upper part of the profile and a zone of well developed, vertical rhizocretions in the lower part (hammer for scale). (b) A bedding plane view of the transverse section of a rhizocretion (pencil for scale). (c) A longitudinal section through a vertically oriented rhizocretion. The slightly tortuous central zone is the void left by decayed root. Tip of the pencil points down.

Table 1
Carbon and oxygen isotopic composition of pedogenic carbonates from Motur, Denwa and Bagra Formations in Central India belonging to Permian, Triassic and Jurassic periods respectively. Also given are calculated $\delta^{18}O$ of meteoric water, calculated $\delta^{13}C$ of soil CO_2 and measured $\delta^{13}C$ of soil organic matter. (The numbers in brackets represent outliers (values more than 2σ from the average) and are not considered for calculation of pCO_2. The numbers in italics represent isotopic composition of spars and are given for comparison with primary micritic values. Carb = carbonate, met. water = meteoric water, and org. = soil organic matter)

Sample	Description	$\delta^{13}C$ (carb.)	$\delta^{18}O_{PDB}$ (carb.)	$\delta^{18}O_{SMOW}$ (carb.)	$\delta^{18}O$ (soil water)[a]	$\delta^{18}O$ (met. water)[a]	$\delta^{13}C$ (soil CO_2)[a]	$\delta^{13}C$ (org)
Motur Formation (260 m.y.)								
M-1	Micrite	−6.3	−10.8	19.8	−9.8	−10.8	−20.8	−23.3
M-2-1	Rhizo-trunk	−6.2	−12.3	18.2	−11.4	−12.4	−20.7	
M-2-2	Rhizo-trunk	−5.1	−12.0	18.5	−11.1	−12.1	−19.7	−23.1
M-2-3	Micrite	−6.2	(−14.4)	(16.0)			−20.7	−23.6
M-2-4	Micrite	−7.0	−12.8	17.7	−11.8	−12.8	−21.5	−23.0
M-2-5	Micrite	−5.7	−12.2	18.3	−11.3	−12.3	−20.3	(−21.9)
M-2-6	Micrite	−5.4	−11.4	19.1	−10.5	−11.5	−20.0	
M-3	Micrite	−6.6	−13.2	17.2	−12.3	−13.3	−21.1	
M-6	Micrite	−7.7	−13.9	16.5	−13.0	−14.0	−22.2	
M-7	Micrite	−7.7	(−8.4)	(22.2)			−22.2	
M-10	Micrite	−7.9	−12.7	17.8	−11.8	−12.8	−22.4	
M-12	Micrite	−5.7	−11.8	18.7	−10.9	−11.9	−20.3	−24.1
M-13	Micrite	−6.9	−12.1	18.4	−11.2	−12.2	−21.4	
M-14	Micrite	−6.7	−12.4	18.0	−11.6	−12.6	−21.2	(−21.4)
M-15	Micrite	−6.2	(−10.3)	(20.2)			−20.7	
M-16	Micrite + Spar	−7.4	(−9.1)	(21.5)			−21.9	
Average		−6.5	−12.3	18.2	−11.4	−12.4	−21.2	−23.5
SD (1σ)		0.8	0.8	0.9	0.8	0.8	0.9	0.5
M-2S	Spar	*−13.3*	*−26.1*	4.0				
M-5	Spar	*−4.6*	*−10.4*	20.1				
M-6S	Spar	*−8.1*	*−17.9*	12.4				
M-8	Spar	*−13.9*	*−23.3*	6.8				(−25.1)
M-9	Spar	*−11.1*	*−12.1*	18.4				−24.0
M-11	Spar	*−4.8*	*−10.2*	20.2				
Denwa Formation (240 m.y.)								
D-2	Micrite	−7.2	−5.5	25.2	−3.5	−4.5	−21.3	
D-3	Micrite	−6.4	−5.5	25.2	−3.5	−4.5	−20.5	
D5-2	Micrite	−6.6	−6.7	24.0	−4.7	−5.7	−20.7	−24.7
D5-3	Micrite	−6.3	−7.0	23.6	−5.0	−6.0	−20.4	(−23.1)
D5-4	Micrite	−7.0	−6.6	24.0	−4.6	−5.6	−21.1	
D5-5	Micrite	−6.7	−5.8	24.9	−3.8	−4.8	−20.8	
D5-6	Micrite	−7.2	−6.7	24.0	−4.7	−5.7	−21.3	
D5-8	Micrite	−7.2	(−10.9)	(19.6)			−21.3	
D5-1	Micrite	−5.8	(−4.6)	26.1			−19.9	
D5-12	Micrite	−6.0	−6.1	24.6	−4.1	−5.1	−20.1	−24.4
D5-16	Micrite	−6.4	(−10.9)	(19.6)	–	–	−20.5	−25.2

Table 1 (*continued*)

Sample	Description	$\delta^{13}C$ (carb.)	$\delta^{18}O_{PDB}$ (carb.)	$\delta^{18}O_{SMOW}$ (carb.)	$\delta^{18}O$ (soil water)[a]	$\delta^{18}O$ (met. water)[a]	$\delta^{13}C$ (soil CO_2)[a]	$\delta^{13}C$ (org)
D-8	Micrite	−7.0	−7.1	23.5	−5.1	−6.1	−21.1	
D-9	Micrite	−6.7	−7.4	23.3	−5.4	−6.3	−20.8	
Average		−6.7	−6.4	24.4	−4.3	−5.3	−20.7	−24.6
SD (1σ)		0.5	0.7	0.9	0.8	0.8	0.5	0.5
D5-15	Micrite + spar							−24.0
D-1	Micrite + spar	*−4.0*	*−2.7*	28.1				
D5-1	Micrite + spar	*−5.9*	*−14.0*	16.4				
D5-7	Micrite + spar	*−4.0*	*−2.9*	27.9				
D5-9	Micrite + spar	*−8.6*	*−6.1*	24.6				
D5-10	spar	*−3.6*	*−2.3*	28.5				(−25.9)
Bagra Formation (200 m.y.)								
B-1	Micrite	−5.4	−6.3	24.4	−4.3	−5.3	−19.5	
B-1-1	Micrite	−6.0	−5.2	25.5	−3.2	−4.2	−20.1	
B-1-4	Micrite	−6.6	−6.3	24.4	−4.3	−5.3	−20.7	
B-1-5	Micrite	−5.7	−7.2	23.4	−5.2	−6.2	−19.8	
B-1-6Lower	Micrite	−5.1	−5.4	25.3	−3.4	−4.4	−19.2	
B-1-6Upper	Micrite	−6.1	−6.8	23.9	−4.8	−5.8	−20.2	−27.5
B-2	Micrite	−6.4	−6.6	24.0	−4.6	−5.6	−20.5	−27.3
B-2-5	Micrite	−4.0	−7.3	23.3	−5.3	−6.3	−18.1	
B-2-6	Micrite	−6.3	−7.2	23.4	−5.2	−6.2	−20.4	
B-2-8	Micrite	−6.2	−6.2	24.4	−4.2	−5.2	−20.0	
B-2-9	Micrite	−5.9	−8.3	22.3	−6.3	−7.3	−20.2	
B-2-10	Micrite	−4.7	−6.6	24.0	−4.6	−5.6	−18.8	
B-3	Micrite	−6.4	−6.4	24.3	−4.4	−5.4	−20.5	
B-4	Micrite	−6.0	−5.6	25.1	−3.6	−4.6	−20.1	
B-5	Micrite	−7.3	−8.0	22.7	−6.0	−7.0	−21.4	
B5-1	Micrite	−5.8	−6.8	23.8	−4.8	−5.8	−19.9	
B5-2	Micrite	−5.1	−5.7	25.0	−3.7	−4.7	−19.2	25.6
B5-3	Micrite	−6.7	−6.5	24.1	−4.5	−5.5	−20.8	
B5-4	Micrite	−6.1	−6.1	24.6	−4.1	−5.1	−20.2	
B5-5	Micrite	−7.3	−7.4	23.3	−5.4	−6.4	−21.4	−24.7
B5-6	Micrite	−6.8	−6.6	24.1	−4.6	−5.6	−20.9	
B5-7	Micrite	−7.0	−6.5	24.1	−4.5	−5.5	−21.1	
B-6	Micrite	−6.1	−5.6	25.0	−3.6	−4.6	−20.2	−25.5
B-7	Micrite	−6.0	−5.8	24.9	−3.8	−4.8	−20.1	
B-8	Micrite	−7.7	−7.0	23.7	−5.0	−6.0	−21.8	

Table 1 (*continued*)

Sample	Description	$\delta^{13}C$ (carb.)	$\delta^{18}O_{PDB}$ (carb.)	$\delta^{18}O_{SMOW}$ (carb.)	$\delta^{18}O$ (soil water)[a]	$\delta^{18}O$ (met. water)[a]	$\delta^{13}C$ (soil CO_2)[a]	$\delta^{13}C$ (org)
Average		−6.1	−6.5	24.1	−4.5	−5.5	−20.2	−26.1
SD (1σ)		0.8	0.8	0.8	0.8	0.8	0.8	1.2
B-1-2	Spar	*−6.0*	*−10.8*	19.7				
B-1-3	Spar	*−6.1*	*−12.1*	18.4				
B-2-3	Spar	*−4.9*	*−10.7*	19.8				
B-2-4	Spar	*−6.2*	*−9.0*	21.6				

[a] These values are calculated assuming soil water in equilibrium with soil carbonate and soil CO_2 at 20°C for Motur and 25°C for Denwa and Bagra soil carbonate respectively. $\delta^{18}C$ values are w.r.t. SMOW and $\delta^{13}C$ w.r.t. PDB.

set of samples. Many of the samples were re-analysed to check the homogeneity of the samples. Isotopic ratios of carbon and oxygen are presented in the usual δ-notation in units of per mil. (‰) with respect to international standard V-PDB and V-SMOW respectively and are reproducible within ±0.1‰ at 1σ level.

4. Results and discussion

The detailed results of isotopic analysis of soil samples are given in Table 1. The mean $\delta^{18}O$ values of the pedogenic carbonate samples from the Motur, Denwa and Bagra Formations (excluding the outliers which deviate by more than 2σ) are 18.2 ($\sigma = 0.9$‰), 24.4 ($\sigma = 0.9$‰) and 24.1‰ ($\sigma = 0.8$‰), respectively. The corresponding mean $\delta^{13}C$ values are −6.5 ($\sigma = 0.8$‰), − 6.7 ($\sigma = 0.5$‰) and −6.1‰ ($\sigma = 0.8$‰). The $\delta^{18}O$ and $\delta^{13}C$ values of all the samples are plotted in a correlation diagram in Fig. 5 which shows that except for a few outliers the values are closely clustered around their respective means. The mean values for pedogenic carbonate samples from the Lameta Formation (Ghosh et al., 1995) are: 24.7‰ for $\delta^{18}O$ and −9.1‰ for $\delta^{13}C$.

The mean $\delta^{13}C$ values of organic matter associated with the palaeosols are: −23.5‰ ($\sigma = 0.5$‰) for the Motur Formation, −24.6‰ ($\sigma = 0.5$‰) for the Denwa Formation and −26.1‰ ($\sigma = 1.2$‰) for the Bagra Formation. Organic matter from a single sample of the Lameta soil yielded a value of −27.6‰. Andrews et al. (1995) reported $\delta^{13}C$ values of −22.1‰ and −17.1‰ for two samples of organic matter from the Lameta Formation. These latter values are somewhat inconsistent with the normal range of C_3 plants and therefore, not considered here.

5. Preservation of geochemical signature

In order to derive palaeoclimatic information from the stable isotopic composition of palaeosol carbonate and organic matter, it is necessary to establish that the samples have not undergone post-depositional alteration. The fine-grained fabric of the samples and the dominance of pedogenic micrites and the absence of sparry calcites in them rule out any major recrystallisation subsequent to the precipitation of original

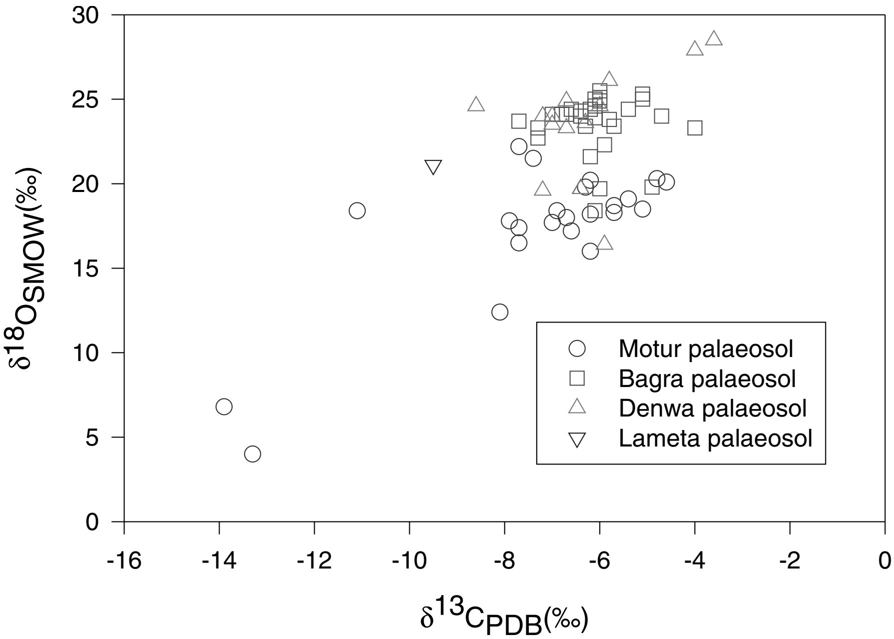

Fig. 5. Plot of $\delta^{18}O$ vs. $\delta^{13}C$ values of the pedogenic carbonates from the Motur, Denwa, Bagra, and Lameta Formations.

carbonate. It is to be noted that microspars are often formed during diagentic alteration. However, they are also occasionally observed in modern vertisols (Referee # 2, private communication). Additionally, the isotopic data show only minor spread in carbon and oxygen isotopic composition (Fig. 5) among various samples from the same Formation (except in a few outliers). The standard deviation of both $\delta^{18}O$ and $\delta^{13}C$ values is within 1‰ and this would be unlikely if alteration affected majority of the samples. It is also to be noted that our results are comparable with the published data of other workers on soil carbonates of similar ages and environments (Cerling, 1991; Yapp and Poths, 1992; Mora et al., 1996).

The observed $\delta^{13}C$ values of the organic matter associated with the pedogenic carbonates lie within a range which closely matches with that of the C_3 vegetative biomass. As all the samples are from horizons older than Miocene when C_4 plants were absent, these values provide additional evidence against any late diagenetic modifications. Moreover, the differences in ($\delta^{13}C$ between coexisting organic matter and carbonate have a range 14–20‰ (see Table 1) similar to that obtained for other palaeosol samples of similar age (Mora et al., 1996).

6. Estimation of atmospheric pCO$_2$

Cerling's (1991) palaeobarometer is basically an isotopic mixing model where the soil-CO_2 is made up of atmospheric CO_2 (through diffusion) and plant-respired CO_2 from vegetative sources. The $\delta^{13}C$ of soil carbonate is governed by the $\delta^{13}C$ value of the soil-CO_2 and fractionation during precipitation which is temperature dependent (Deines et al., 1974). The $\delta^{13}C$ values of the two sources of soil-CO_2 are quite different. Whereas the recent pre-industrial atmospheric CO_2 is -6.5‰, the CO_2 respired by C_3 type vegetation can have value between -20 and -35‰, with a mean around -27‰ (Ehleringer, 1989). The degree of infiltration of the atmospheric CO_2 in the soil matrix (which is dependent on the atmospheric pCO_2) thus influences the $\delta^{13}C$ value of the soil-CO_2 and consequently the $\delta^{13}C$ value of the pedogenic carbonate. Therefore, this model allows us to estimate the pCO_2 values of the ancient atmosphere from the $\delta^{13}C$ values of the pedogenic carbonates if the following parameters are known:

(a) The temperature of calcite precipitation in the soil.

(b) The $\delta^{13}C$ value of the plant-respired CO_2.
(c) The $\delta^{13}C$ value of the atmospheric CO_2.
(d) The difference between the soil pCO_2 and the atmospheric pCO_2.

We discuss below the procedure for estimating each of these parameters.

(a) *Temperature of calcite precipitation*. The temperature of calcite precipitation in a soil is close to the mean soil surface temperature. Scotese (1998) surmised that the Permian was a period during which large global temperature changes took place. In the Early Permian global temperature was low with a mean around 10°C and at the end of the Permian the temperature was extremely high near about 35°C (Scotese, 1998). The global temperature was maintained at a slightly reduced value of 30°C till the Middle Jurassic. The wide spread glacial deposits at the Permo-Carboniferous boundary (Talchir Formation) followed by thick coal deposits of the overlying Barakar Formation (Fig. 1), the occurrence of red beds and calcic palaeosols in the Motur, Denwa and Bagra Formations and the presence of thick deposits of carbonaceous claystones in the Bijori Formation (Late Permian) together corroborate the suggested trend of the global temperature. However, the surface temperature of a locality is also influenced by its altitude and its latitudinal position. The palaeogeographic reconstructions of the Gondwana landmasses indicate that the study area was situated at 60°S during the Permian (260 m.y.), at 45°S during the Middle Triassic (240 m.y.) and at 25°S during the Middle Jurassic (200 m.y.). During this period the altitude seems to have remained consistently low and probably close to the sea level (Scotese, 1997).

In this study temperature of soil carbonate precipitation is inferred based on palaeosol character and comparison with modern analogues. The palaeosols described in this study were formed in palaeolatitudes corresponding to modern temperate and arid climate. Modern growing season temperature at sea level in similar latitudes typically ranges from 10 to 30°. A plot of maximum monthly temperature suitable for calcrete formation for the 60–25°S latitudes reveal that, for the modern condition 20°C is a typical temperature at 60°S latitude while it is 25°C at 45° S and 25°S, respectively (Ekart et al., 1999). We have therefore chosen 20°C as the temperature of soil carbonate precipitation during Permian (260 m.y.), Motur formation and 25°C for Triassic (240 m.y.), Denwa and Middle Jurassic (200 m.y.) Bagra Formations (Table 2).

(b) *$\delta^{13}C$ value of the plant-respired CO_2*. The $\delta^{13}C$ values of the organic matters associated with the soils have been determined in this study and can be considered as the proxy for the $\delta^{13}C$ of plant-respired CO_2. Prior to the Miocene, C_4 plants were not present in the ecosystem and C_3 plants were the dominant vegetative biomass. The $\delta^{13}C$ values of the plant-respired CO_2 of the modern C_3 plants range from −20 to −35‰ with an average of −27‰ (Ehleringer, 1989). The mean $\delta^{13}C$ values of −23.5, −24.6, −26.1 and −27.6‰ for the Motur, Denwa, Bagra and Lameta Formations (Table 1) lie close to the mean $\delta^{13}C$ of the modern C_3 plants and provide robust estimates of the plant-respired CO_2 values at those times.

(c) *$\delta^{13}C$ value of the atmospheric CO_2*. The $\delta^{13}C$ of atmospheric CO_2 is an important input in Cerling's model and needs to be estimated independently. In earlier studies (Cerling, 1991; Andrews et al., 1995; Ghosh et al., 1995) the $\delta^{13}C$ was assumed to be constant and its value was taken to be −6.5‰ equal to the pre-industrial atmospheric CO_2 value. However, since then several studies (Mora et al., 1996; Thackeray et al., 1990) have demonstrated variation in the $\delta^{13}C$ of atmospheric CO_2 in the past. There are two ways of estimating this $\delta^{13}C$; one based on $\delta^{13}C$ of marine brachiopods (Mora et al., 1996) and the other based on $\delta^{13}C$ of organic matter (Farquhar et al., 1989; Thackeray et al., 1990). Since the brachiopod data (Veizer et al., 1986) show a large variation we adopt the second alternative here. The mean $\delta^{13}C$ of the C_3 organic matter in modern environment is about 21‰ depleted compared to the $\delta^{13}C$ of the atmospheric CO_2. A similar relationship has been noted for the Late Palaeozoic and Early Cretaceous periods (Mora et al., 1996; Grocke et al., 1999). Using this value of depletion and the measured $\delta^{13}C$ value of organic matter associated with the palaeosols one can estimate the $\delta^{13}C$ of the contemporary atmospheric CO_2.The mean $\delta^{13}C$ of the organic matter from the Motur, Denwa, Bagra and Lameta Formations are −23.5, −24.6, −26.1 and −27.6‰, respectively

Table 2
Estimation of concentration of atmospheric CO_2 and its isotopic composition at different times in the past.

Formation (Age in m.y.)	$\delta^{13}C$ (carb.)[a]	Temperature[b] (°C)	$\delta^{13}C$ (OM)	$\delta^{13}C$ (atmospheric CO_2)[c]	pCO_2[d]		Mean concentration of atmospheric CO_2 (ppmV)
					A	B	
Motur (260)	−6.5	20	−23.5	−2.5	540	890	715
Denwa (240)	−6.7	25	−24.6	−3.6	910	1510	1210
Bagra (200)	−6.1	25	−26.1	−5.1	1675	2775	2225
Lameta (65)	−9.1	25	−27.6	−6.6	1110	1850	1480

[a] From Table 1.
[b] Temperature estimates from IAEA/WMO, 1998 as quoted in Ekart et al. (1999).
[c] $\delta^{13}C$ of atmospheric CO_2 obtained by subtracting 21‰ from $\delta^{13}C$ (OM) (see text).
[d] Columns A and B refer to S_z values of 3000 and 5000 ppm in Cerling's model (see text).

(Table 1). Therefore, the $\delta^{13}C$ values of the atmospheric CO_2 in those periods are estimated to be −2.5, −3.6, −5.1 and −6.6‰, respectively. It is interesting to note that there is systematic decrease in the $\delta^{13}C$ from 260 to 65 m.y.

(d) *Difference between the soil pCO_2 and the atmospheric pCO_2: S_z parameter.* The difference in concentration between the soil CO_2 and the atmospheric CO_2 depends on soil porosity, soil respiration rate and the depth of CO_2 production. This difference (S_z) plays an important role in Cerling's mixing model and needs to be assessed independently. Approximate value of the soil porosity can be obtained from observations made on recent soils of the same type. However, the mean CO_2 production depth and the soil respiration rate for geologically ancient soils cannot be estimated with certainty. The rooting depth, the dimensions of the rhizoliths and their density of occurrence in the palaeosol profiles may probably be used for such estimation but no such model is available at present. Observations made on the modern soils show that for the desert soils S_z is less than 3000 ppmV and for well-drained temperate and tropical soils S_z ranges between 5000 and 10,000 ppmV. Mora et al. (1996) assumed a value between 3000 and 7000 ppmV for the Middle to Late Palaeozoic semi-arid tropical to temperate vertic palaeosols. Some of these palaeosols (of Silurian age) indicate a very shallow rooting depth. On the other hand, Ghosh et al. (1995) adopted a range between 3000 and 5000 ppmV for the well-drained semi-arid Late Cretaceous palaeosols with higher rooting depths than the Silurian soils (Ghosh et al., 1995; Tandon et al., 1995, 1998; Ghosh, 1997). We note that the gleyed pedohorizons (signature of clay rich component with less permeability) are, in general, absent in the profiles of the Denwa, Bagra and Lameta Formations. Some amount of gleying is present close to the Bk pedohorizons of the Motur and the Denwa Formations that may suggest a higher value of S_z. However, high latitudinal position (60°S) of the study area along with low mean annual temperature during the Motur time implies reduced plant productivity and consequently low S_z. All the palaeosols analysed in this work show characteristics of well-drained, semi-arid soils. In view of the above considerations, a range of S_z values between 3000 and 5000 ppmV is adopted for these palaeosols.

7. The CO_2 palaeobarometry

Using the mean $\delta^{13}C$ values of the palaeosol carbonates along with above mentioned values of the required parameters and estimated $\delta^{13}C$ of the atmospheric CO_2 based on soil organic matter in the model of Cerling (1991) we obtain following range of pCO_2 values (in ppmV): 540–890 for the Motur period, 910–1510 for the Denwa period, 1675–2775 for the Bagra period and 1110–1850 for the Lameta period (Table 2). The estimate for the Late Cretaceous is higher compared to the range 800–1200 ppmV deduced in our earlier study (Ghosh et al., 1995) which was based on an assumed value of −26‰ for the $\delta^{13}C$ of plant-respired CO_2 in contrast to −27.6‰ as measured and assumed in the present study. The uncertainties in average $\delta^{13}C$ (OM) (see Table 1) is not included in the quoted uncertainty of the pCO_2. However, variations in $\delta^{13}C$ (OM) as given in Table 1 (0.5‰ for Motur and Denwa and 1.2‰ for Bagra formation) would change the calculated mean pCO_2 by 20% for Motur and Denwa and 40% for Bagra Formation respectively. It is to be noted that the soil samples studied here belong to the same geochemical milieu as they all formed in the same basin at different time; therefore, the relative CO_2 variation is expected to be well constrained.

These values represent first independent estimates of atmospheric CO_2 level during 260–200 m.y. from the soils formed in the (southern hemisphere) Gondwana supercontinent. This is considered an important period in the evolution model which predicts an increase in the CO_2 level after the Early Permian low (310–285 m.y.) and ascribes it to enhanced rate of degassing. This prediction is verified by our results but the detailed nature of variation is found to be slightly different. Fig. 6 shows a plot of CO_2 concentration in ppmV against soil age (in m.y.). It is seen that there is excellent agreement of derived concentration with Berner's prediction for 260 and 240 m.y. (Motur and Denwa) but the abundance of CO_2 for 200 m.y. (Bagra) and 65 m.y. (Lameta) are 2225 ppmV and 1480 ppmV in contrast to Berner's mass balance model estimates of about 1400 and 560, respectively. The disagreement persists even at the lower limit of our estimate. The parameters involved in the calculation of pCO_2 during the Bagra and Lameta time are well constrained and therefore, the high CO_2 level seems to be genuine. Fig. 6 also shows recent compilation of new data and previously published values by earlier workers given in Ekart et al. (1999). A curve showing weighted running average of calculated pCO_2 assuming 25°C as soil temperature is superimposed in Fig. 6 for comparison. It is seen that the derived concentration from soil carbonates for Motur formation (260 m.y.) is less than other estimates. However, concentration for Denwa (240 m.y.), Bagra (200 m.y.) and Lameta (65 m.y.) Formations show close agreement with observations made by other workers.

8. Oxygen isotope composition of soil water

Isotopic composition of soil-water can be derived from the isotopic composition of oxygen in pedogenic carbonates if the temperature of calcium carbonate precipitation can be estimated independently. As explained above, surface temperatures at the time of deposition of Motur, Denwa and Bagra sediments are estimated from palaeo-latitude of the sampling location (using reconstruction of Scotese, 1997) and modern day surface temperature observations at different latitudes published by IAEA (1998). The estimated temperature during deposition of Motur sediments is 20°C while it is around 25°C during deposition of Denwa and Bagra sediments. The $\delta^{18}O$ values of water in equilibrium with pedogenic carbonates are calculated assuming these temperatures and using Friedman and O'Neil (1977) equation. The results (Table 1) show that the expected oxygen isotopic composition of the soil water during the Motur time (260 m.y.) ranges from −9.8 to −13.0‰ (w.r.t SMOW) while it ranges between −3.5 to −5.4‰ for Denwa and −3.2 to −6.3‰ for Bagra Formations (240 and 200 m.y., respectively).

The composition of meteoric water during the above periods can be derived from that of soil-water if the effect of evaporation is taken into account. However, there is uncertainty in the extent of evaporative enrichment during transformation of meteoric water to soil-water. Salomons et al. (1978) estimated a value of 1‰ for this effect in contrast to 4‰ enrichment obtained by Quade et al. (1989) for arid soils in Nevada. The mean $\delta^{18}O$ values of the soil water for Motur, Denwa and Bagra sediments are: −11.4, −4.3

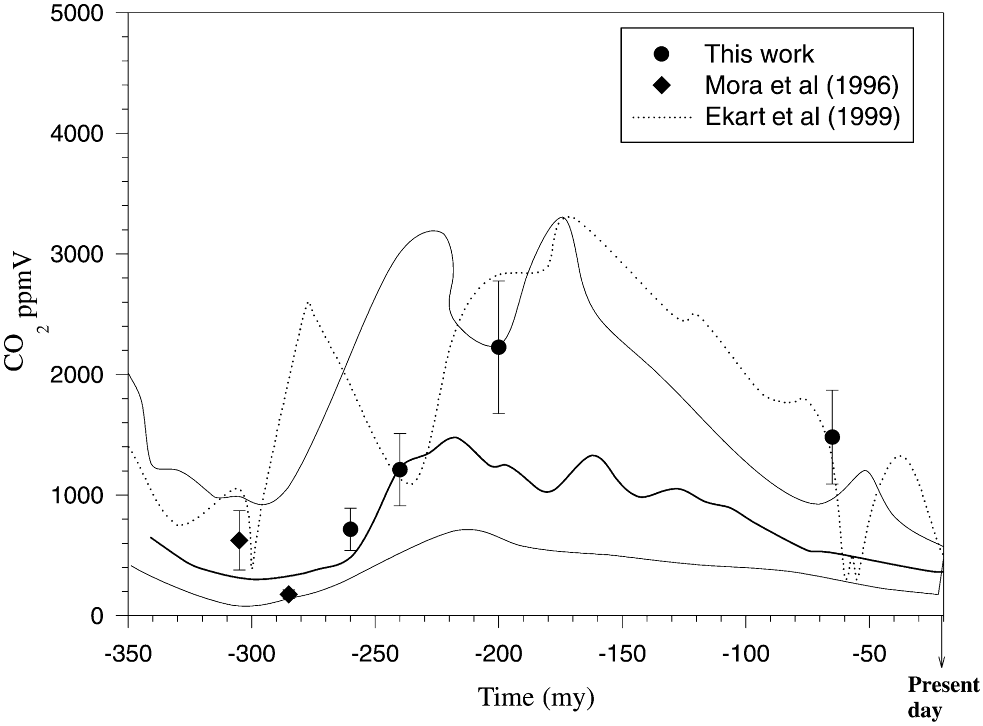

Fig. 6. Estimated concentration of atmospheric CO_2 as a function of time. The points are based on isotopic analysis of pedogenic carbonates. The curve shown by the solid line along with envelope (range of uncertainty) is obtained from Berner (1997). The dotted curve represents the paleo-pCO_2 estimates from compilation by Ekart et al. (1999).

and −4.5‰ (w.r.t. SMOW), respectively. This variation is consistent with the latitudinal variation in modern day precipitation as observed in the IAEA compilation of isotopic values of rainwater in different island stations (IAEA/WMO Report, 1998) situated at 60, 45 and 25° S latitudes with $\delta^{18}O$ values of −12, −5 and −5‰, respectively. Therefore, the observed changes in the composition of rainwater from Motur to Bagra time can be explained by northward movement of the Indian plate subsequent to the breakup of Gondwanaland during 260–200 m.y.

9. Conclusions

Four sets of soil horizons have been discovered in the Gondwana strata of Central India, which developed in the Motur, Denwa, Bagra and Lameta Formations of Satpura basin. All these soils have well formed pedogenic carbonates. Soil carbonates from several horizons of these formations were analysed for oxygen and carbon isotopic ratios to infer the environment of precipitation and estimate the concentration of CO_2 in the atmosphere using Cerling's model. The concentration of CO_2 was low (~715 ppmV) during the Early Permian (260 m.y.) followed by continuous rise during Middle Triassic (~1210 ppmV at 240 m.y.) and Jurassic (~2225 ppmV at 200 m.y.) (Table 2). This period was followed by a decline to ~1480 ppmV during the Cretaceous. The general feature of the variation in CO_2 level found in this study is consistent with Berner's model prediction. However, the Mid-Jurassic and Cretaceous levels seem to be much higher than the predicted concentration. The rapid increase in CO_2 is also consistent with field observation of the soil maturity from the three stratigraphic levels. Since this study is based on soils developed in the same basin and therefore, same geochemical milieu the relative variation over time is well constrained. The $\delta^{13}C$ of the atmospheric CO_2 is inversely related to the concentration in this period suggesting enhanced role of degassing from Earth's interior. Such increased degassing is expected from rapid break-up of Gondwana landmass during this time.

References

Andrews, J.E., Tandon, S.K., Dennis, P.F., 1995. Concentration of carbon dioxide in the Late Cretaceous atmosphere. J. Geol. Soc. Lond. 152, 1–3.

Bandyopadhyay, S., Sengupta, D.P., 1998. Middle Triassic vertebrate from India. (abs.) Gondwana 10, Cape Town. J. Afr. Earth Sci. 27 (1987), 16–17.

Barnola, J.M., Raynaud, D., Korotkevitch, Y.S., Lorius, C., 1987. Vostok ice core: a 160,000 years record of atmospheric CO_2. Nature 329, 408–414.

Berner, R.A., 1991. A model for atmospheric CO_2 over Phanerozoic time. Am. J. Sci. 291, 339–376.

Berner, R.A., 1993. Paleozoic atmospheric CO_2: importance of solar radiation and plant evolution. Science 261, 68–70.

Berner, R.A., 1994. GEOCARB II: a revised model of atmospheric CO_2 over Phanerozoic time. Am. J. Sci. 294, 56–91.

Berner, R.A., 1997. The rise of plants and their effect on weathering and atmospheric CO_2. Science 276, 544–545.

Casshyap, S.M., Qidwai, H.A., 1971. Paleocurrent analysis of Lower Gondwana sedimentary rocks, Pench Valley Coalfield, Madhya Pradesh (India). 5, pp. 135–145.

Casshyap, S.M., Tewari, R.C., 1988. Depositional model and tectonic evolution of Gondwana basins: Lucknow. The Palaeobotanist 36, 59–66.

Casshyap, S.M., Tewari, R.C., Khan, A., 1993. Alluvial fan origin of the Bagra Formation (Mesozoic Gondwana) and tectono-stratigraphic implications. J. Geol. Soc. India 42, 269–279.

Cerling, T.E., 1991. Carbon dioxide in the atmosphere: evidence from Cenozoic and Mesozoic palaeosols. Am. J. Sci. 291, 377–400.

Chatterjee, S., RoyChowdhury, T., 1974. Triassic Gondwana vertebrates from India. Indian J. Earth Sci. 11, 96–112.

Deines, P., Langmuir, D., Harmon, R.S., 1974. Stable carbon isotope ratios and existence of a gas phase in the evolution of carbonate ground waters. Geochim. Cosmochim. Acta 38, 1147–1164.

Driese, S.G., Mora, C.I., 1993. Physico-chemical environment of pedogenic carbonate formation in Devonian vertic palaeosols, central appalachians, USA. Sedimentology 40, 199–216.

Ehleringer, J.R., 1989. Carbon isotope ratios and physiological processes in arid land plants. In: Rundel, P.W., Ehleringer, J.R., Nagy, K.A. (Eds.), Applications of Stable Isotopic Ratios to Ecological Research. Springer, New York.

Ekart, D.D., Cerling, T.E., Montanez, I.P., Tabor, N.J., 1999. A 400 million year carbon isotope record of pedogenic carbonate: implications for paleoatmospheric carbon dioxide. Am. J. Sci. 299, 805–827.

Farquhar, G.D., Ehleringer, J.R., Hubick, K.T., 1989. Carbon isotope discrimination and photosynthesis. Annual Review of Plant Physiology and Plant Molecular Biology 40, 503–537.

Ghosh, P., 1997. Geomorphology and palaeoclimatology of some Upper Cretaceous palaeosols in central India. Sedim. Geol. 110, 25–49.

Ghosh, P., Bhattacharya, S.K., Jani, R.A., 1995. Palaeoclimate and palaeovegetation in central India during the Upper Cretaceous based on stable isotope composition of the palaeosol carbonates. Palaeogeogr. Palaeoclimatol. Palaeoecol. 114, 285–296.

Ghosh, P., Rudra, D.K., Maulik, P., 1998. Palaeoclimatic indicators in the Satpura Gondwana succession, India, Gondwana 10. J. Afr. Earth Sci. 27, 1A.

Grocke, D.R., Hesselbo, S.P., Jenkyns, H.C., 1999. Carbon-isotope composition of Lower Cretaceous fossil wood: ocean-atmosphere chemistry and relation to sea-level changes. Geology 27, 155–158.

Houghton, R.A., Wood, G.M., 1989. Global climate change. Sci. Am. 260, 36–44.

IAEA/WMO Report, 1998. The GNIP database, Release 2. Global network for isotopes in precipitation, International Atomic Energy Agency.

Keeling, C.D., 1994. Global historical CO_2 emissions. In: Boden, T.A., Kaiser, D.P., Sepanski, R.J., Stoss, F.W., Logsdon, F.W. (Eds.), Trends'93: A Compendium of Data on Global Change. American Geological Institute, Springfield, VA, pp. 501–505.

Keeling, C.D., Worf, T.P., 1998. Atmospheric CO_2 concentrations — Mauna Loa Observatory, Hawaii, 1958–1997, http://cdiac.esd.ornl.gov/ftp/ndp001/maunaloa.co2.

Keeling, C.D., Piper, S.C., Heimann, M., 1989. A three dimensional model of atmospheric CO_2 transport based on observed winds: 4, mean annual gradients and inter annual variations. In: Peterson, D.H. (Ed.), Aspects of Climate Variability in Pacific and Western America. Geophysical Monograph, vol. 55. AGU, Washington, pp. 305–363.

Maulik, P.K., Chakraborty, C., Ghosh, P., Rudra, D., 2000. Meso- and macro-scale architecture of a Triassic fluvial succession: Denwa Formation, Satpura Gondwana Basin, Madhya Pradesh. J. Geol. Soc. India 56, 489–516.

McElwain, J.C., Chaloner, W.G., 1996. The fossil cuticle as a skeletal record of environmental change. Palaios. 11, 376–388.

Mora, C.I., Fastovsky, D.E., Driese, S.G., 1993. Geochemistry and stable isotopes of palaeosols. A Geological Society of America Continuing Education Short Course, 66pp.

Mora, C.I., Driese, S.G., Colarusso, L.A., 1996. Middle to Late Paleozoic atmospheric CO_2 levels from soil carbonate and organic matter. Science 271, 1105–1107.

Mora, C.I., Sheldon, B.T., Elliott, C.W., Driese, S.G., 1998. An oxygen isotope study of illite and calcite in three Appalachian Paleozoic vertic paleosols. J. Sedim. Res. 68, 456–464.

Mukherjee, R.N., Sengupta, D.P., 1998. New capitosaurid amphibians from the Middle Triassic Denwa Formation of Satpura Gondwanas, Central India. Alcheringa 22, 317–327.

Quade, J., Cerling, T.E., Bowman, J.R., 1989. Systematic variations in the carbon and oxygen isotopic composition of pedogenic carbonate along elevation transects in the southern Great Basin, United States. Geol. Soc. Am. Bull. 101, 464–475 (with suppl. Data 89-10).

Raja Rao, C.S. (Ed.), 1983. Coalfields of India: coal resouces of Madhya Pradesh, Jammu and Kashmir. GSI Bull. 3, pp. 195–198.

Robinson, P.L., 1967. The Indian Gondwana formations — a review. In: Amos, A.J. (Ed.), Gondwana Stratigraphy, International Union of Geological Sciences Symposium, Buenos Aires, October 1–15, 1967. United Nations Educational, Scientific, and Cultural Organizations, Paris, pp. 201–268.

Salomons, W., Goudie, A., Mook, W.G., 1978. Isotope composition of calcrete deposits from Europe, Africa and India. Earth Surf. Proc. 3, 43–57.

Sarkar, A., Ramesh, R., Bhattacharaya, S.K., 1990. Effect of sample pretreatment and size fraction on the $\delta^{18}O$ and $\delta^{13}C$ values of foraminifera in Arabian sea sediments. Terra Nova 2, 489–493.

Satsangi, P.P., 1988. Vertebrate fauna from the Indian Gondwana Sequence: Lucknow. The Paleobotanist 36, 245–253.

Scotese, C.R., 1997. Paleogeographic Atlas, PALEOMAP Progress Report 90-0497, Department of Geology, University of Texas at Arlington, Arlington, Texas.

Scotese, C.R., 1998. Gondwana's climate changes. J. Afr. Earth Sci. 27, 172–173 (abstracts).

Soil Survey Staff, 1975. Soil Taxonomy: A basic system of soil classification for making and interpreting soil surveys. Soil Conserv. Surv. Handbook, 436. Washington DC, US Department of Agriculture.

Tajika, E., Matsui, T., 1992. Evolution of terrestrial proto-CO_2 atmosphere coupled with thermal history of the earth. Earth Planet. Sci. Lett. 113, 251–266.

Tandon, S.K., Sood, A., Andrews, J.E., Dennis, P.F., 1995. Palaeoenvironments of the dinosaur-bearing Lameta Beds (Maastrichtian), Narmada Valley, Central India. Palaeogeogr. Palaeoclimatol. Palaeoecol. 117, 123–154.

Tandon, S.K., Andrews, J.E., Sood, A., Mittal, S., 1998. Shrinkage and sediment supply control on multiple calcrete profile development: a case study from the Maastrichtian of central India. Sedim. Geol. 119, 25–45.

Thackeray, J.F., van der Merwe, N.J., Thorp-Lee, J.A., Sillen, A., Lanham, J.L., Smith, R., Keyser, A., Monteiro, P.M.S., 1990. Changes in carbon isotope ratios in the late Permian recorded in the therapsid tooth apatite. Nature 347, 751–753.

Veevers, J.J., Tewari, R.C., 1995. Gondwana Master Basin of peninsular India between Tethys and the interior of the Gondwanaland province of Pangea. Mem. Geol. Soc. Am. 187, 1–72.

Veizer, J., Fritz, P., Jones, B., 1986. Geochemistry of brachiopods: oxygen and carbon isotopic records of Paleozoic oceans. Geochim. Cosmochim. Acta 50, 1679–1696.

Yapp, C.J., Poths, H., 1992. Ancient atmospheric CO_2 pressures inferred from natural goethites. Nature 355, 342–344.